ELSEVIER

Biophysical Chemistry 58 (1996) 215–224

Biophysical Chemistry

Simulation of oxidative phosphorylation in hepatocytes

Bernard Korzeniewski

Institute of Molecular Biology, Jagiellonian University, al. Mickiewicza 3, 31-120 Kraków, Poland

Received 16 July 1994; revised 22 March 1995; accepted 23 May 1995

Abstract

The dynamic mathematical model of oxidative phosphorylation proposed previously was modified, developed and further tested. The description of cytochrome oxidase kinetics was changed to involve dependence on Δp. Simple, phenomenological descriptions of the kinetics of substrate dehydrogenation and ATP usage, able to reflect experimental data correctly, were found. The kinetic response of the oxidation subsystem (substrate dehydrogenation, respiratory chain), phosphorylation subsystem (ATP synthase, ATP/ADP carrier, phosphate carrier, ATP usage) and proton leak to the changes of Δp in isolated hepatocytes incubated with different respiratory substrates was simulated. The simulations revealed a good agreement with the experimental results. Simple, intuitive assumptions were able, when introduced into the model, to explain differences in the properties of the oxidative phosphorylation system working with different respiratory substrates. It was proposed, therefore, that our explicit understanding of the oxidative phosphorylation system was good enough to explain many properties of this system correctly, at least in the range of physiological conditions tested.

Keywords: Oxidative phosphorylation; Dynamic model; Computer simulation; Metabolic control analysis; Metabolic regulation

1. Introduction

The mathematical model of a sophisticated biochemical system (pathway) contrary to many physical theories, cannot describe the considered system with very great accuracy and be valid for very great range of conditions, since the number of parameters to be taken into account is enormous. Such a model is never completed as it can be extended for an increasing range of conditions and subsequently involve an increasing amount of parameters. However, it is not advantageous to consider as many parameters and conditions as possible because of limitations of our knowledge and difficulties with an operation on a very large number of data. Therefore it is necessary to determine the conditions which are the most interesting and useful for biochemists, the parameters and boundaries of the considered system (other conditions can be neglected and other parameters kept constant).

The most natural boundary (giving the best isolation of a system) for the oxidative phosphorylation process is the cell surface. The isolated mitochondria system is much more difficult, since it does not contain natural substrate dehydrogenation and ATP usage processes. The most interesting parameters are those important for control and regulation of the cell energy metabolism, and which are involved in the response to external signals. These parameters are concentrations of 'key' bioenergetic intermediate metabolites (ATP/ADP, proton-motive force (Δp), NAD^+/NADH) and sensitivities of different enzymes (processes) for them, also called elasticities in metabolic control analysis [10,11]. The relevant con-

SSDI 0301-4622(95)00077-1

ditions include different concentrations of respiratory substrates and oxygen (and other external effectors, like hormones) present in a physiological incubation medium.

The purpose of this paper is to develop a mathematical dynamic model of oxidative phosphorylation in isolated hepatocytes incubated with different respiratory substrates, being able to simulate correctly the energetic behaviour of the cell during great variations of the respiration rate and Δp (and other relevant parameters). Since the model of oxidative phosphorylation [1–3] developed and verified earlier fulfils most of the above mentioned requirements (it simulates correctly, for example, flux control coefficients for different parts of the system and time courses of different parameters during the aerobiosis → anaerobiosis transition); only a slight modification of this model is necessary.

The description of the cytochrome oxidase kinetics in the previous model [1–3] was based on the steady-state model developed by Wilson, Erecińska and others [4–6]. It contained a dependence on the external ATP/ADP*P_i ratio and assumed that the ATP/ADP carrier worked near the equilibrium. Therefore it was outdated from the point of view of recent knowledge [7]. The modified model should include the direct dependence of the cytochrome oxidase kinetics on Δp. Some minor changes of the model are also required to reflect the experimental data more accurately.

Very good quantitative experimental data concerning the whole cell bioenergetic behaviour were obtained in the frame of the 'top-down' approach [8,9] to the metabolic control analysis [10–12]. This approach deals with biochemical subsystems rather than with single enzymes. In the cited papers the oxidative phosphorylation system was divided into three subsystems: the oxidation subsystem (substrate dehydrogenation, respiratory chain), the phosphorylation subsystem (ATP synthase, ATP/ADP carrier, phosphate carrier and ATP usage) and the proton leak subsystem (proton leak alone), linked with each other by a 'common metabolite' Δp. Kinetic responses of all three subsystems to Δp were measured in a broad range of the respiration rate and Δp in isolated hepatocytes for different respiratory substrates (glucose, fatty acids, lactate/pyruvate) using specific inhibitors [8,9]. These data seem to be very useful to serve as the reference for modifying and testing of the model.

The previous model [2,3] predicted correctly the values of the flux control coefficients [10,11] of the three distinguished subsystems over the oxidation, phosphorylation and proton leak fluxes, measured experimentally in the cited papers. However, these simulations concerned explicitly a near neighbourhood of the 'physiological point' (state $3_{1/2}$). The aim of the present work is to extent the comparison of computer simulations with the experimental results discussed to the whole range of the changes in the respiration rate and Δp tested.

2. Model

The dynamic model of oxidative phosphorylation developed previously [2,3] was slightly modified to be in accordance with present knowledge and to get a better fit to experimental results. Kinetic descriptions of particular reactions (processes) of oxidative phosphorylation are presented in Table 1. They represent dependencies of particular reaction rates on concentrations of different metabolites and/or on thermodynamic forces. Changes in time of particular metabolite concentrations are expressed as a set of differential equations, presented in Table 2 (for detailed description see ref. [2] and [3]). These changes are the result of a balance between the rates of the reactions producing and consuming a particular metabolite.

As in ref. [3], three modes of the work of cells (hepatocytes) were distinguished:

Mode 1, β-oxidation of fatty acids as the source of reducing equivalents, fatty acids as a respiratory substrate, no additional ATP supply (glycolysis), only 'basal' ATP consumption (protein synthesis, ion transport).

Mode 2, glycolysis as a source of reducing equivalents and additional ATP supply, glucose as a respiratory substrate, only 'basal' ATP utilisation.

Mode 3, lactate as a respiratory substrate, no additional ATP supply, gluconeogenesis as the main ATP-consuming process (additional to the 'basal' ATP consumption).

The modifications of the model presented in the previous papers [2,3] are indicated below.

Table 1
Kinetic descriptions of particular enzymes (processes) of oxidative phosphorylation. The details are given in the text or in refs. [2] and [3]

Cytochrome oxidase
$$v_{COX} = k_{COX} \cdot a^{2+} \cdot c^{2+}/(1 + K_{m_{O_2}}/O_2)$$

Respiratory chain (complex I and III)
$$v_{CHAIN} = k_{CHAIN} \cdot \Delta G_{CHAIN}$$

Substrate dehydrogenation
$$v_{DEHY} = V_{DEHY}/(1 + K_{m_D}(NAD^+/NADH))^{P_e}$$

Proton leak
$$v_{LEAK} = k_{L1}(e^{k_{L2} \cdot \Delta\Psi} - 1) + k_{L3} \cdot \Delta p$$

ATP synthase
$$v_{SYNT} = k_{SYNT}(\gamma - 1)/(\gamma + 1), \gamma = 10^{\Delta G_{SYNT}/RT}$$

ATP/ADP carrier
$$v_{EXCH} = k_{EXCH}\left(\frac{ADP_{fe}}{ADP_{fe} + ATP_{fe} \cdot 10^{\Psi_e/Z}} - \frac{ADP_{fi}}{ADP_{fi} + ATP_{fi} \cdot 10^{\Psi_i/Z}}\right)$$
$$k_{EXCH} = k^*_{EXCH} \cdot 10^{\Delta G_{EXCH}/Z \cdot P_a}$$

Phosphate carrier
$$v_{PIIN} = k_{fP} \cdot H_e \cdot P_{i_e} - k_{bP} \cdot H_i \cdot P_{i_i}$$

ATP utilisation
$v_{UTIL} = V_{UTIL}/(1 + K_{mU}/ATP_{te})$ in Mode 1 and 2
$v_{UTIL} = k_{UTIL} \cdot ATP_{te}/ADP_{te}$ in Mode 3

Glycolysis
$$v_{GLYC} = k_{GLYC} \cdot AMP_{te}/ATP_{te}$$

Adenylate kinase
$$v_{ADKN} = k_{fA} \cdot ADP_{me} \cdot ADP_{fe} - k_{bA} \cdot ATP_{me} \cdot AMP_e$$

Table 2
The set of differential equations used in calculations. In Mode 2 the rate of glycolysis is also involved. R_{cm}, the ratio of cell volume to mitochondria volume, R_{sc}, the ratio of suspension volume to cell volume, r_{buff}, buffering capacity for protons

Oxygen	$\dot{O}_2 = -v_{COX}$
Reduced form of cytochrome c	$\dot{c}^{2+} = v_{CHAIN} - 4 \cdot v_{COX}$
NADH	$\dot{NADH} = v_{DEHY} - 0.5 \cdot v_{CHAIN}$
Internal protons	$\dot{H}_i = -(8(2 + 2u)v_{COX} + 2(2 - 2u)vC_{CHAIN} - u \cdot v_{EXCH} - (1 - u)v_{PIIN} - v_{LEAK} \cdot R_{cm} \cdot R_{sc}/r_{buff}$
External protons	$\dot{H}_e = -\dot{H}_i/R_{cm}$
Internal ATP	$\dot{ATP}_{ti} = (v_{SYNT} - v_{EXCH}) \cdot R_{cm} \cdot R_{sc}$
Internal ADP	$\dot{ADP}_{ti} = -\dot{ATP}_{ti}$
Internal inorganic phosphate	$\dot{P}_{i_i} = (v_{PIIN} - v_{SYNT}) \cdot R_{cm} \cdot R_{sc}$
External ATP	$\dot{ATP}_{te} = (v_{EXCH} + v_{ADKN} - v_{UTIL}) \cdot R_{sc}$
External ADP	$\dot{ADP}_{te} = (v_{UTIL} - 2 \cdot v_{ADKN} - v_{EXCH}) \cdot R_{sc}$
External AMP	$\dot{AMP}_e = v_{ADKN} \cdot R_{sc}$
External inorganic phosphate	$\dot{P}_{i_e} = (v_{UTIL} - v_{PIIN}) \cdot R_{sc}$

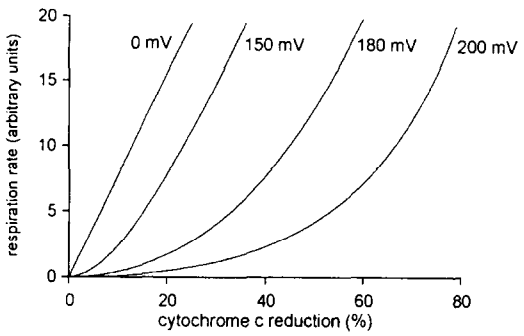

Fig. 1. Simulated dependence of the respiration rate on Δp and cytochrome c reduction level. The presented curves are obtained for four different values of Δp. In the 'physiological state' cytochrome c is reduced in about 20% and the value of Δp is about 180 mV.

2.1. Cytochrome oxidase

The previous description of this enzyme [1], based on the steady-state model developed by Wilson, Erecińska and others [4–6], was profoundly modified. The model was greatly simplified and the dependence on the external ATP/ADP*P ratio was replaced with the dependence on Δp. The only property of the original model which has remained unchanged was the two-electron reduction of oxygen. The rate expression for the cytochrome oxidase (v_{COX}) used in this paper is:

$$v_{COX} = k_{COX} \cdot a^{2+} \cdot c^{2+} / \left(1 + K_{mO_2}/O_2\right) \qquad (1)$$

where a^{2+} is the reduced form of the oxygen-binding centre (cyt. $a_3 + Cu^B$), c^{2+} is the reduced form of cytochrome c and $K_{mO_2} = 12$ μM is the Michaelis–Menten constant for oxygen. A mid-point redox potential value for cytochrome c equal to 250 mV was accepted and the mid-point redox potential for the oxygen-binding centre equal to 540 mV was calculated to obtain the reduction level of this centre in state 3 equal to about 7%, which is comparable with the cytochrome a_3 reduction level (5–10% [13]). The reduction level of the oxygen-binding centre was calculated from the following equation (assuming the existence of near-equilibrium between cytochrome c, the oxygen-binding centre and Δp, although it can be valid only approximately):

$$Z \cdot \log\left(a^{3+}/a^{2+}\right) = \Delta p \cdot (1 + u) + E_{mc} + Z \cdot \log\left(c^{3+}/c^{2+}\right) - E_{ma} \qquad (2)$$

where u was constant and equal to $\Delta\Psi/\Delta p$ and E_m the mid-point redox potential.

Fig. 1 shows the calculated dependence of the cytochrome oxidase reaction rate on the cytochrome c reduction level for four different values of Δp. The curves obtained in the simulations are similar to the experimental curves of the dependence of the respiration rate on the cytochrome c reduction level for different values of the external phosphorylation potential [6]. At higher cytochrome c reduction levels, the simulated curves for higher values of Δp tend to be more bent upward, towards greater values of the respiration rate than the experimental curves for higher external phosphorylation potentials, as could be expected from displacement of the ATP/ADP carrier from equilibrium (thermodynamic separation of Δp and the external phosphorylation potential) at higher values of the respiration rate.

Fig. 2 shows the simulated time course of the cytochrome c reduction level during aerobiosis →

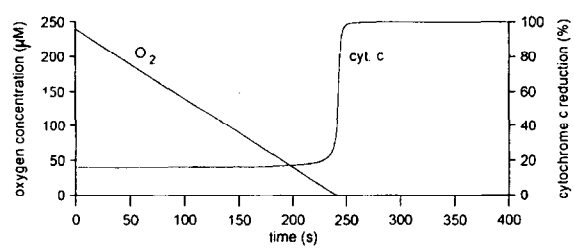

Fig. 2. Simulated time courses of oxygen concentration and reduction level of cytochrome c in suspension of isolated hepatocytes during aerobiosis → anaerobiosis transition.

anaerobiosis transition (consumption of oxygen in a closed chamber to zero) in suspension of isolated hepatocytes. The curve for cytochrome c exhibits even greater similarity to experimental results [14] than an analogous curve obtained using the earlier model [2] (steeper bend when oxygen concentration reaches zero). The apparent Michaelis–Menten constant for oxygen obtained in simulations is less than 1 μM (about 0.5 μM), which is in accordance with the experiments [15]. The 'real' Michaelis–Menten constant used in the simulations is much greater (12 μM). This suggests a very important role of the changing cytochrome c reduction level and Δp in the compensation of changes in the oxygen concentration in order to keep the respiration rate as constant as possible. The presented results suggest that the proposed simplified description of cytochrome oxidase is a good enough approximation.

2.2. Substrate dehydrogenation

The description of the substrate dehydrogenation process proposed in the previous paper [3] was also slightly simplified. In the present publication the following expression was used:

$$\nu_{DEHY} = V_{DEHY}/\left(1 + K_{mD}(NAD^+/NADH)\right)^{P_e}. \quad (3)$$

where the Michaelis–Menten constant K_{mD} is equal to 20. In Mode 3 V_{DEHY} was enlarged to obtain an increase of the respiration rate by 50% and Δp by about 5 mV comparing with Modes 1 and 2 [16]. The value of the power expression P_e, determining sensitivity of substrate dehydrogenation to the $NAD^+/NADH$ ratio, is different in different modes. In Mode 1 some redox equivalents (NADH and $FADH_2$) are supplied directly from β-oxidation, which is probably less sensitive to this ratio than Krebs cycle. Therefore, relatively low value of P_e (0.18) was assumed. In Mode 2 all redox equivalents come from the Krebs cycle, which is efficiently regulated by the $NAD^+/NADH$ ratio. For this reason, the value of P_e is higher in this case (0.35). In Mode 3 much NADH is produced by lactate dehydrogenase working near equilibrium and therefore being very sensitive to this ratio. Therefore, in this case the value of P_e is the highest (0.5).

2.3. Proton leak

The proton leak description was the same as in [3]:

$$\nu_{LEAK} = k_{L1}(e^{k_{L2}\cdot\Delta\Psi} - 1) + k_{L3}\cdot\Delta p \quad (4)$$

with the following constants for Modes 1 and 2:

$k_{L1} = 9.2\cdot10^{-7}\,\mu M\,H^+\,s^{-1}$

$k_{L2} = 9.4\cdot10^{-2}\,mV^{-1}$

$k_{L3} = 1.5\cdot10^{-2}\,\mu M\,H^+\,mV^{-1}\,s^{-1}$,

and for Mode 3:

$k_{L1} = 5.5\cdot10^{-2}\,\mu M\,H^+\,s^{-1}$

$k_{L2} = 3.0\cdot10^{-2}\,mV^{-1}$

$k_{L3} = 2.4\cdot10^{-2}\,\mu M\,H^+\,mV^{-1}\,s^{-1}$

The values of the coefficients were adjusted to mimic experimental results. Differences between Modes 1, 2 and Mode 3 can reflect real differences or experimental variability. In the latter case, the parameter values for all three modes would be the same and probably in between the values used for Modes 1 and 2, and Mode 3.

2.4. ATP / ADP carrier

The description of the ATP/ADP carrier from the previous paper [2] was slightly modified. The appropriate rate expression was clarified by a simple mathematical transformation. The meanings of Ψ_i and Ψ_e were changed. In the cited paper these terms denoted internal and external membrane potentials, respectively. However, since there is little physical sense in the separation of the 'components' of $\Delta\Psi$, the terms mentioned were reinterpreted as 'effective' components of $\Delta\Psi$ with respect to the transport of adenine nucleotides from inside and from outside of mitochondria, catalysed by the ATP/ADP carrier. Ψ_e was estimated to be equal to $0.35\cdot\Delta\Psi$ on the basis of relative uptake of ATP and ADP by mitochondria [17], and $\Psi_i = \Delta\Psi - \Psi_e$. The final expression for the ATP/ADP carrier velocity is:

$$\nu_{EXCH} = k_{EXCH}\left(\frac{ADP_{fe}}{ADP_{fe} + ATP_{fe}\cdot10^{\Psi_e/Z}} - \frac{ADP_{fi}}{ADP_{fi} + ATP_{fi}\cdot10^{\Psi_i/Z}}\right) \quad (5)$$

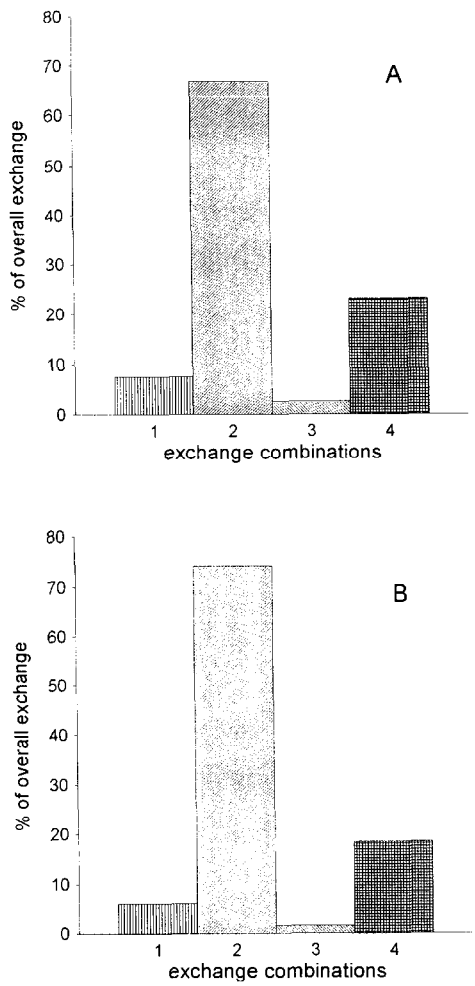

Fig. 3. Experimental (A) and simulated (B) relative rates of four combinations of exchange of ATP and ADP by the ATP/ADP carrier: 1, external ADP for internal ADP, 2, external ADP for internal ATP, 3, external ATP for internal ADP, 4, external ATP for internal ATP.

where subscript 'f' is free. This equation allows a correct description of the relative distribution of four combinations of exchange of adenine nucleotides. Fig. 3 shows a comparison of computer simulations based on the considered model (Fig. 3B) with the experimental results for isolated mitochondria [18] (Fig. 3A). The picture obtained is similar in both cases. The predominant exchange combination is the transport of ADP inside and ATP outside mitochondria. The opposite exchange is more than 20 times slower. Some difference between the experimental and theoretical results can be due to slightly different membrane potentials and external Mg^{2+} concentrations.

Nevertheless, in the above description, the carrier velocity is saturated for about 80% in state $3_{1/2}$. Therefore the equation presented is able to describe correctly the distribution of exchange combinations only but not a stimulation of the net exchange rate. A modification of this description is necessary. It was introduced by a substitution of the rate constant k_{EXCH} with the expression $k_{EXCH} \cdot 10^{\Delta G_{EXCH}/Z \cdot P_a}$, where P_a was adjusted to be equal to 0.3. This description has been tested in a broad range of conditions (this paper and the accompanying paper).

2.5. ATP utilisation

The reactions of 'basal' ATP consumption (protein synthesis, ion transport) are supposed, as crucial for keeping the cell alive, to be relatively independent of ATP (and ADP) concentration. Therefore, the following simple equation was used for a description of the external ATP utilisation in Modes 1 and 2:

$$\nu_{UTIL} = V_{maxU}/(1 + K_{mU}/ATP_{te}) \quad (6)$$

where $K_{mU} = 300$ μM and subscript 't' is total. According to this equation, the ATP usage process is almost saturated with ATP at physiological concentrations of this compound.

The rate of gluconeogenesis was reported to be very sensitive (in absence of glucagon and other hormones) to the ATP/ADP ratio (the dependence being nearly linear). For this reason, a linear dependence of ATP consumption on the ATP/ADP ratio was used in Mode 3:

$$\nu_{UTIL} = k_{UTIL} \cdot ATP_{te}/ADP_{te}. \quad (7)$$

The k_{UTIL} constant value was adjusted to cause an increase of the respiratory rate by 50% and Δp by 5 mV comparing with Modes 1 and 2 [16].

2.6. Glycolysis

Phosphofructokinase, the main rate-controlling enzyme in glycolysis was reported to be efficiently activated by AMP and inhibited by ATP. Therefore,

the glycolytic ATP supply was described in Mode 2 by the following simple equation:

$$\nu_{GLYC} = k_{GLYC} \cdot AMP_{te}/ATP_{te}. \quad (8)$$

The value of k_{GLYC} was adjusted to obtain a production of about 10% of ATP directly from glycolysis in the 'physiological' point.

2.7. Numerical procedures

The set of differential equations described in the previous papers [2,3] and modified as mentioned above (see also Tables 1 and 2), was being integrated by means of the Gear subroutine. Calculations were performed utilizing the Microsoft FORTRAN programming language. The simulations were performed on a PC/386 (33 MHz) computer equipped with coprocessor.

3. Results and discussion

Since absolute values of the mitochondrial membrane potential (or Δp) and the respiration rate for similar conditions differ somewhat in different experiments [8,9,16], in the present paper relative values of these parameters are used. In the simulations performed 100% of $\Delta\Psi$ (Δp) corresponds to 155 mV (182 mV) in Modes 1 and 2 and to about 160 mV (188 mV) in Mode 3. 100% of the respiration rate is equivalent to about 1 nmol O_2 mg wet mass^{-1} min^{-1} in Modes 1 and 2 [8,16] and 1.5 nmol O_2 mg wet mass^{-1} s^{-1} in Mode 3 [9,16]. In the simulations a linear dependence between $\Delta\Psi$ and Δp was assumed [19,20].

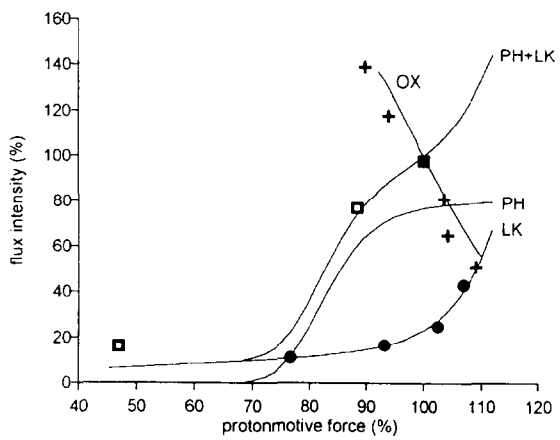

Fig. 4. Experimental points and simulated curves representing kinetic responses of the oxidation, phosphorylation and proton leak subsystems to Δp in Mode 1 in hepatocytes. The experimental points are taken from [8]. OX, oxidation flux, PH, phosphorylation flux, LK, proton leak flux, ■, physiological point, +, oxidation subsystem titration, □, phosphorylation + proton leak subsystem titration. ●, proton leak subsystem titration.

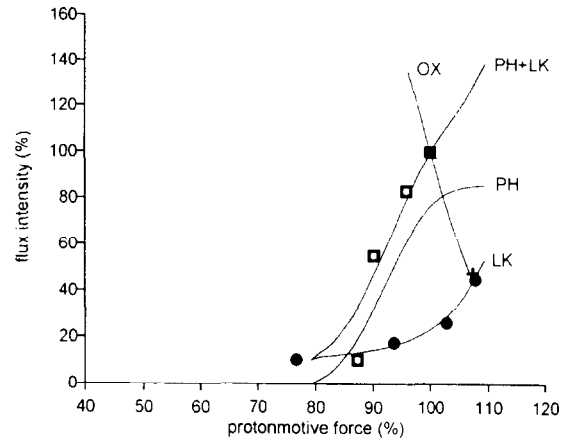

Fig. 5. Experimental points and simulated curves representing kinetic responses of the oxidation, phosphorylation and proton leak subsystems to Δp in Mode 2. The experimental points are taken from [8]. OX, oxidation flux, PH, phosphorylation flux, LK, proton leak flux, ■, physiological point, +, oxidation subsystem titration, □, phosphorylation + proton leak subsystem titration, •, proton leak subsystem titration.

The simulated kinetic responses of the oxidation, phosphorylation and proton leak subsystems to Δp in Mode 1 are compared with the experimentally measured kinetic responses of these subsystems to Δp for hepatocytes isolated from starved rats (Fig. 5 in [8]) in Fig. 4. A good agreement between the simulations and the experimental results can be observed. The simulated curves reflect well the kinetic responses of the oxidation, proton leak and proton leak + phosphorylation subsystems to Δp, obtained by titration of the system with oligomycin, myxothiazol in the presence of excess of oligomycin, and myxothiazol, respectively. An explicitly shown dependence of the phosphorylation subsystem on Δp is an additional information. However, the theoretical results, being consistent with the experimental

data mentioned, do in some details not agree with their interpretation presented in [8]. The authors fit a straight line to the three points representing the kinetic response of the phosphorylation + proton leak subsystem to Δp (Fig. 5 in [8]). Of course, this is the simplest possibility. Nevertheless, the simulations suggest that a more complicated case occurs and the dependence is significantly non-linear. There is additional evidence that this theoretical result is correct. The phosphorylation flux is of course a result of the subtraction of the proton leak flux from the phosphorylation + proton leak flux at the same value of Δp. In the cited experimental paper only two latter fluxes were measured directly and the phosphorylation flux was calculated using the mentioned subtraction. If we extrapolate the hypothetical linear dependence of the phosphorylation + proton leak flux on Δp to the respiration rate and Δp values higher than 100%, we will obtain that the phosphorylation flux decreases with an increase of Δp. This of course would be highly improbable and therefore the linear dependence of the phosphorylation + proton leak flux on Δp cannot be accepted. For this reason, the elasticity coefficient of the phosphorylation subsystem to Δp calculated in the discussed paper [8] on the basis of the linear fit mentioned, is probably overestimated, as was discussed previously [3]. It represents only a 'large scale' and not a real elasticity of the phosphorylation subsystem to Δp. The simulations suggest that the kinetic response of the phosphorylation subsystem to Δp is sigmoidal and that at the 'physiological point' (100% of Δp and the respiration rate) the phosphorylation flux is almost completely saturated with Δp. Therefore this flux cannot be significantly stimulated by a rise in Δp (for example through a direct stimulation of the oxidation subsystem). It is interesting that above about 75% of the physiological value of Δp the sum of dependencies of the phosphorylation flux and the proton leak flux on Δp is near linear, although dependencies of the two separated fluxes on Δp are strongly non-linear.

Fig. 5 shows a comparison of the simulated and experimentally measured (Fig. 4 in [8]) kinetic responses of the three considered subsystems to Δp in Mode 2 (hepatocytes from fed rats; glycolysis as an additional source of ATP supply). Again, a quite good agreement can be observed. In comparison with Mode 1, the additional ATP supply from glycolysis increases the phosphorylation subsystem sensitivity to Δp. This is caused by buffering of the changing ATP/ADP ratio by changes in the glycolytic ATP production. The additional ATP supply allows the maintenance of a higher value of Δp at the same respiration rate, when the oxidation subsystem is inhibited. This is possible, as the glycolytic flux is very sensitive to the ATP/AMP ratio and therefore to the ATP/ADP ratio (ADP concentration is related to AMP concentration through adenylate kinase). However, at lower values of the respiration rate and Δp, the predictions of the model are somewhat different from the experimental results. The probable reason is an oversimplified description of the kinetics of the glycolytic pathway. The other possible reason is discussed together with the discussion of Mode 3. In Mode 2, like in Mode 1, the dependence of the sum of the phosphorylation and proton leak fluxes on Δp is near-linear above about 80% of the physiological value of Δp, while dependencies of particular subsystems on Δp are strongly non-linear.

Mode 3 (hepatocytes incubated in the presence of lactate and pyruvate) is an 'active' mode of the cell work, as the respiration rate is increased by about 50% and Δp by about 5 mV in relation to Modes 1 and 2 [16]. In Fig. 6 the simulated kinetic responses of the three discussed subsystems to Δp in Mode 3 are compared with the experimental kinetic responses measured for hyperthyroid-paired euthyroid

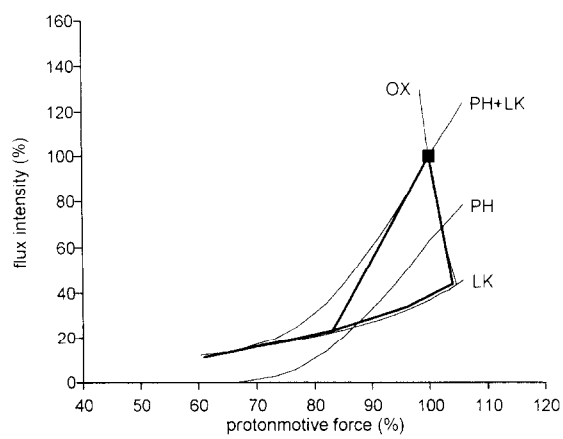

Fig. 6. Experimental (thick lines) and simulated (thin lines) curves representing kinetic responses of the oxidation, phosphorylation and proton leak subsystems to Δp in Mode 3. The experimental curves are taken from [9].

hepatocytes incubated with lactate and pyruvate (Fig. 5 in [9]). Generally, a good agreement can be observed. The simulated and experimental curves of the oxidation and proton leak subsystem dependencies on Δp are very similar. The simulated phosphorylation + proton leak flux has somewhat greater intensity than the experimental one at lower values of Δp. The first reason, like in Mode 2, is not a very accurate description of the phosphorylation subsystem (especially the description of the ATP consumption). However, there is also another possible explanation of this discrepancy. The experimental results for both Mode 2 (Fig. 5 in [8]) and Mode 3 (Fig. 5 in [9]) exhibit an enigmatic property. At low values of Δp the sum of phosphorylation flux and proton leak flux intensities is smaller than an intensity of the proton leak flux alone. This paradox suggests that the measurements of the respiration rate and/or Δp at low Δp values involve some systematic errors. Therefore it is possible that the simulations reflect the real situation at lower values of Δp more accurately than the experiments mentioned. If we accept these experimental results and analyse the kinetic response of the phosphorylation subsystem to Δp (obtained by subtraction of the proton leak flux from the phosphorylation + proton leak flux for each value of Δp), we will conclude that the phosphorylation flux is very sharply 'turned off' at a certain value of Δp (about 85% of the physiological value). It would be difficult to find a kinetic mechanism responsible for such a 'violent' regulation.

The sensitivity of the phosphorylation subsystem to Δp is greater in Mode 3 than in Mode 1 (compare Figs. 4 and 6). The simulations performed suggest that the greater sensitivity of the ATP usage to the ATP/ADP ratio is a possible explanation of this phenomenon. Because lactate + pyruvate stimulate a gluconeogenetic flux which strongly depends on this ratio, this is in fact probable. Similarly, the observed increased sensitivity of the oxidation subsystem to Δp in Mode 3 can be explained by an increased sensitivity of the substrate dehydrogenation process to the NAD^+/NADH ratio.

One of the main questions arising is: is the observed agreement between simulations and experiments an evidence for validity and usefulness of the model? The model operates on a very large number of parameters and there is a possibility that the agreement with experimental data can be achieved simply by manipulation with parameter values. However, most of these values are taken from the literature or calculated from the reported experimental data. The accepted kinetic descriptions of the ATP/ADP carrier and cytochrome oxidase were tested in the present paper and, to a much greater extent, in the accompanying paper. The kinetic expressions for substrate dehydrogenation and ATP usage were adjusted to mimic the experimental results. However, even they were semi-quantitatively based on our knowledge, as mentioned in the description of the model. Moreover, explicit, although phenomenological, descriptions of these processes found, provide us some net information. For example, we can conclude that the dependencies of substrate dehydrogenation on NAD^+/NADH and ATP usage on ATP/ADP are between linearly proportional and saturated (and not, for example, sigmoidal). This is in agreement with our knowledge, concerning different NADH-producing and ATP-consuming reactions.

There is another evidence that the discussed model is at least useful. The previous version of the model [3] (but the present version produced the same results) predicted that Ca^{2+}-acting hormones (as vasopressin, adrenaline and glucagon) activated Δp-producing and Δp-consuming reactions to a very similar extent, contrary to some intuitive expectations [7] that only Δp-producing reactions were stimulated. The experiment projected to test this prediction [16] confirmed the theoretical results obtained using the model. In fact, many quantitative predictions cannot be made intuitively because of the complexity of the considered systems and limitations of the human brain. The model can be, at least in principle, 'falsified', which is the main requirement for any scientific 'theory'. Of course, it should be tested for more sets of experimental data and modified, if necessary. This is the main aim of the present (and the accompanying) paper.

The earlier developed model of the oxidative phosphorylation system [1–3] was modified in the present paper. The reason was a need for consistency with our recent knowledge about this system. The outdated model of the cytochrome oxidase kinetics was changed to involve the dependence on Δp. The new model is much simpler and reflects experimen-

tal results in a better way. Furthermore, it allows to appreciate explicitly the role of changes in the cytochrome c reduction level and Δp in compensation of the decrease of the oxygen concentration during the aerobiosis → anaerobiosis transition in order to keep the respiration rate as constant as possible (the 'apparent' Michaelis–Menten constant for oxygen is over 20 times lower than the 'real' one, see above). The description of the ATP/ADP carrier was slightly changed to clarify its physical interpretation. The new description suggests that the kinetic mechanisms analysed by Klingenberg [17,18] are responsible mainly for the relative distribution of the four combinations of the exchange of ATP and ADP, but not for changes in the net ATP and ADP transport. The latter are likely to be due a modification of an overall carrier activity rather than to a change in the relative distribution of the exchange combinations. Of course this supposition should be checked experimentally.

The other aim of the present paper was to further test the modified model by comparison with the experimental results. This was done by simulation of the kinetic responses of the oxidation, phosphorylation and proton leak subsystems to Δp for different modes of the cell work. The test was successful, showing a good agreement with experiments. Of course, some kinetic parameters were adjusted to obtain such an agreement. Descriptions of some enzymes (processes) were more or less phenomenological. However, if we are able to derive the sophisticated pattern of the behaviour of the whole oxidative phosphorylation system from the properties of its components in a broad range of conditions, we can assume that we have at least approximately correct knowledge both about particular components and the entire system. The explicit testing of the discussed model is not limited to the present paper. All the theoretical results and predictions obtained by use of the earlier version of the model [2,3] are still valid, at least semiquantitatively, for the new model. Furthermore, after an adjustment to isolated mitochondria conditions, the model is able to simulate the behaviour of oxidative phosphorylation in a broad range of conditions very well (see the accompanying paper). Finally, simple intuitive mechanisms are able, when incorporated to the model, to explain the differences between the three distinguished modes of cell work. Therefore, we can trust that it is not by mere chance but through our understanding of the function of the oxidative phosphorylation system that the testing of the model was successful.

Acknowledgements

This work was supported by Komitet Badań Naukowych.

References

[1] B. Korzeniewski and W. Froncisz, Studia Biophys., 132 (1989) 173–187.
[2] B. Korzeniewski and W. Froncisz, Biochim. Biophys. Acta, 1060 (1991) 210–223.
[3] B. Korzeniewski and W. Froncisz, Biochim. Biophys. Acta, 1102 (1992) 67–75.
[4] D.F. Wilson, C.S. Owen and A. Holian, Arch. Biochem. Biophys., 182 (1977) 749–762.
[5] D.F. Wilson, C.S. Owen and M. Erecińska, Arch. Biochem. Biophys., 195 (1979) 494–504.
[6] D.F. Wilson and D. Nelson, in J. Eisenfeld and C. DeLisi (Editors), Mathematics and Computers in Biomedical Application, Elsevier, Amsterdam, 1985, pp. 119–124.
[7] M.D. Brand and M.P. Murphy, Biol. Rev., 62 (1987) 141–193.
[8] G.C. Brown, P.L. Lakin-Thomas and M.D. Brand, Eur. J. Biochem., 188 (1990) 313–319.
[9] M.-E. Harper and M.D. Brand, J. Biol. Chem., 268 (1993) 14850–14860.
[10] H. Kacser and J. Burns, Symp. Soc. Exp. Biol., 27 (1973) 65–107.
[11] R. Heinrich and T.A. Rapoport, Eur. J. Biochem., 42 (1974) 107–120.
[12] H. Kacser and J.W. Porteous, TIBS, 12 (1987) 5–14.
[13] S. Papa, in T.E. King, H.S. Mason and M. Morrison (Editors), Oxidases and Related Redox Systems, Alan L. Liss, New York, 1988.
[14] T. Kashiwagura, D.F. Wilson and M. Erecińska, J. Cell. Physiol., 120 (1984) 13–18.
[15] D.F. Wilson and M. Erecińska, CHEST, 88 (1985) 229s–232s.
[16] B. Korzeniewski, M.-E. Harper and M.D. Brand, Biochim. Biophys Acta, in press.
[17] M. Klingenberg, J. Membrane Biol., 56 (1980) 97–105.
[18] M. Klingenberg, in A.N. Martinosi (Editor), The Enzymes of Biological Membranes, vol. 4, Plenum Press, New York, 1985.
[19] J. Duszyński, K. Bogucka and L. Wojtczak, Biochim. Biophys. Acta, 767 (1984) 540–547.
[20] J.G. Reich and K. Rohde, Biomed. Biochim. Acta, 42 (1983) 37–46.,